Electrical Stimulation of the Frontal Eye Fields in the Head-Free Macaque Evokes Kinematically Normal 3D Gaze Shifts

Jachin A. Monteon, Alina G. Constantin, Hongying Wang, Julio Martinez-Trujillo and J. Douglas Crawford

J Neurophysiol 104:3462-3475, 2010. First published 29 September 2010;
doi: 10.1152/jn.01032.2009

Journal of Neurophysiology publishes original articles on the function of the nervous system. It is published 12 times a year (monthly) by the American Physiological Society, 9650 Rockville Pike, Bethesda MD 20814-3991.
 ISSN: 0022-3077, ESSN: 1522-1598. Visit our website at http://www.the-aps.org/.

J Neurophysiol 104: 3462–3475, 2010.
First published September 23, 2010; doi:10.1152/jn.01032.2009.

Electrical Stimulation of the Frontal Eye Fields in the Head-Free Macaque Evokes Kinematically Normal 3D Gaze Shifts

Jachin A. Monteon,[1,2,3] Alina G. Constantin,[1,2] Hongying Wang,[1,2] Julio Martinez-Trujillo,[5] and J. Douglas Crawford[1,2,3,4]

[1]*Centre for Vision Research,* [2]*Canadian Action and Perception Network,* [3]*Department of Biology, and* [4]*Department of Psychology and School of Kinesiology and Health Sciences, York University, Toronto, Ontario; and* [5]*Department of Physiology, McGill University, Montreal, Quebec, Canada*

Submitted 23 November 2009; accepted in final form 28 September 2010

Monteon JA, Constantin AG, Wang H, Martinez-Trujillo J, Crawford JD. Electrical stimulation of the frontal eye fields in the head-free macaque evokes kinematically normal 3D gaze shifts. *J Neurophysiol* 104: 3462–3475, 2010. First published September 23, 2010; doi:10.1152/jn.01032.2009. The frontal eye field (FEF) is a region of the primate prefrontal cortex that is central to eye-movement generation and target selection. It has been shown that neurons in this area encode commands for saccadic eye movements. Furthermore, it has been suggested that the FEF may be involved in the generation of gaze commands for the eye and the head. To test this suggestion, we systematically stimulated (with pulses of 300 Hz frequency, 200 ms duration, 30–100 μA intensity) the FEF of two macaques, with the head unrestrained, while recording three-dimensional (3D) eye and head rotations. In a total of 95 sites, the stimulation consistently elicited gaze-orienting movements ranging in amplitude from 2 to 172°, directed contralateral to the stimulation site, and with variable vertical components. These movements were typically a combination of eye-in-head saccades and head-in-space movements. We then performed a comparison between the stimulation-evoked movements and gaze shifts voluntarily made by the animal. The kinematics of the stimulation-evoked movements (i.e., their spatiotemporal properties, their velocity–amplitude relationships, and the relative contributions of the eye and the head as a function of movement amplitude) were very similar to those of natural gaze shifts. Moreover, they obeyed the same 3D constraints as the natural gaze shifts (i.e., modified Listing's law for eye-in-head movements). As in natural gaze shifts, saccade and vestibuloocular reflex torsion during stimulation-evoked movements were coordinated so that at the end of the head movement the eye-in-head ended up in Listing's plane. In summary, movements evoked by stimulation of the FEF closely resembled those of naturally occurring eye–head gaze shifts. Thus we conclude that the FEF explicitly encodes gaze commands and that the kinematic aspects of eye–head coordination are likely specified by downstream mechanisms.

INTRODUCTION

Primates analyze detailed retinal images by reorienting them toward the fovea. These reorientations are normally achieved through head-free gaze shifts (i.e., coordinated movements of the eyes, head, and body; Crawford et al. 1999; Freedman and Sparks 1997; Guitton 1992; McCluskey and Cullen 2007; Tomlinson and Bahra 1986a).

Gaze shifts are movements of the eyes relative to space (Es) and usually have two components: movements of the head relative to space (Hs) and movements of the eyes relative to head (Eh) (Crawford et al. 1999; Freedman and Sparks 1997; Guitton 1992; Tomlinson and Bahra 1986a). A typical gaze shift consists of a fast Eh movement (saccade), followed by an Hs movement with a slower velocity. Es reaches the target first and, as the head turns, the Eh is proportionally reduced in size by the vestibuloocular reflex (VOR) to impede gaze overshoot (Bizzi et al. 1971; Guitton 1992; Tomlinson and Bahra 1986b). During large gaze shifts (>40°) movements of the body relative to space also make a significant contribution to the gaze shift (McCluskey and Cullen 2007). One important question in gaze control is how discrete brain areas implement cephalomotor and oculomotor commands to execute these coordinated movements. The purpose of the current study was to examine the role of the frontal eye field (FEF) in gaze control.

The FEF is a region of the prefrontal cortex involved in eye-movement generation (Bruce and Goldberg 1985; Bruce et al. 1985) and target selection (Schall et al. 1995a; Trageser et al. 2008). Single-unit recordings have shown that the FEF plays a role in the transformation of visual signals into saccade motor commands (Schall 1997) and in the selection of visual targets (Schall and Thompson 1999). In addition, it has been shown that the activity of many neurons in the FEF is modulated around the time of saccades, with a specific magnitude and direction, and that a topographic representation of saccade vectors exists across the FEF (Bruce and Goldberg 1985; Bruce et al. 1985). In humans, functional magnetic resonance imaging studies have shown that the bold signal in the FEF is correlated with visually guided saccade generation (Burke and Barnes 2008). Likewise, transcranial magnetic stimulation of the FEF can disrupt saccade generation (Nyffeler et al. 2006). Moreover, it was recently demonstrated that the human FEF represents both retinal locations and extraretinal locations behind the head (Tark and Curtis 2009).

Supporting these observations, anatomical studies in monkeys have shown that the FEF receives visual inputs from the thalamus and possesses extensive reciprocal connectivity with visual cortical areas (Huerta et al. 1987; Schall et al. 1995b; Stanton et al. 1995). It also has a direct pathway (Segraves 1992) to the brain stem premotor circuitry for eye and head movements (Sparks and Hartwich-Young 1989) and an indirect pathway to these circuits via the superior colliculus (SC) (Komatsu and Suzuki 1985; Sommer and Wurtz 2000).

Electrical microstimulation has proved to be an important tool for investigating FEF function (Bruce et al. 1985; Moore and Armstrong 2003; Murphey and Maunsell 2008; Robinson and Fuchs 1969). Although microstimulation has the advantage

Address for reprint requests and other correspondence: J. D. Crawford, Department of Psychology, York University, 4700 Keele St., Toronto, ON, Canada, M3J 1P3 (E-mail: jdc@yorku.ca).

of showing a causal link between particular brain areas and behavior, it has the disadvantage that we still know little about how brain circuits respond to it. (Histed et al. 2009; Ranck Jr 1975; Tehovnik et al. 2006). Thus it is perhaps best to consider microstimulation as a *perturbation*, where the brain site, task, and stimulation parameters are the independent variables and the dependent variable—the behavioral response—provides an indirect measure of the brain's overall response to this perturbation.

In the case of the FEF, microstimulation evokes short-latency saccades in head-restrained monkeys (Bruce et al. 1985; Robinson and Fuchs 1969; Schiller and Sandell 1983) and rapid coordinated movements of the eyes and the head in head-unrestrained monkeys (Chen 2006; Elsley et al. 2007; Knight and Fuchs 2007; Sparks et al. 2001; Tu and Keating 2000). Some reports have suggested that the FEF could encode separate eye and head commands (Chen 2006); other reports, that it encodes gaze commands composed of coordinated eye and head movements (Elsley et al. 2007; Knight and Fuchs 2007; Tu and Keating 2000). These two views have led to a controversy that so far has not been clarified. Another caveat is that the activation pattern of the underlying neck muscles evoked by electrical stimulation of the FEF differs from the activation pattern in volitional gaze shifts, suggesting different control mechanisms (Elsley et al. 2007).

One way to shed further light onto this issue would be examining whether eye and head movements produced by stimulation of the FEF obey the three-dimensional (3D) constraints (around the horizontal, vertical, and torsional axes) of naturally coordinated gaze shifts (Constantin et al. 2009; Klier et al. 2003; Martinez-Trujillo et al. 2003b). Donders' law states that for every possible two-dimensional (2D) gaze direction, the eyes possess a fixed amount of torsion about a nasooccipital axis (Donders 1848). When the head is fixed, a special form of Donders' law, Listing's law, is obeyed (Crawford et al. 2003; Ferman et al. 1987a,b; Tweed and Vilis 1990; von Helmholtz 1867). Listing's law states that when the head is fixed, the eyes assume only those orientations that can be reached from a central reference position by rotation about axes that lie in a plane. As a result, the torsional angle of the eyes relative to that plane is always zero. During fixations between natural head-free gaze shifts in human subjects (Glenn and Vilis 1992; Radau et al. 1994) and monkeys (Crawford and Vilis 1991; Crawford et al. 1999), similar laws are obeyed. The head follows a form of Donders' law called the Fick strategy, whereas the eyes-in-head follow Listing's law. However, to achieve the latter, precise eye–head coordination is necessary because many times the brain must predict the amount of torsion produced by the vestibuloocular reflex (VOR) during the final "slow phase" of the movement (Crawford and Vilis 1991; Crawford et al. 1999; Tweed 1997).

Some brain circuits for gaze control appear to be robust enough to respond to microstimulation with normal 3D behavior, depending on the site of stimulation. For example, microstimulation of the supplementary eye field (SEF) and the SC—considered upstream and downstream from the FEF, respectively—generates gaze saccades with normal patterns of 3D eye–head coordination (Klier and Crawford 2003; Martinez-Trujillo et al. 2003b). In contrast, microstimulation of reticular formation oculomotor structures in the midbrain produces torsional eye and head movements that do not obey Donders' law (Crawford et al. 2003; Klier et al. 2007). Moreover, microstimulation of the lateral intraparietal area (LIP), which also projects into the FEF (Andersen et al. 1985; Huerta et al. 1987; Schall et al. 1995b; Stanton et al. 1995), fails to evoke large head movements (Brotchie et al. 1995; Constantin et al. 2009; Thier and Andersen 1998) and evokes eye movements with unnatural torsional components (Constantin et al. 2009). Thus natural/unnatural 3D movements can be evoked from structures both up- and downstream from the FEF and thus one can not assume, one way or the other, what will happen during FEF stimulation. The present study aims to clarify this issue by providing a detailed analysis of the kinematics of eye and head movements generated during FEF stimulation and comparing them with the kinematics of naturally occurring movements.

The central question to our study is: does electrical stimulation of the FEF result in normally coordinated gaze shifts (i.e., where gaze is shifted through normal combinations of behaviorally natural motion of the eye and head)? We chose three criteria that have been used in similar investigations of gaze coding in head-free monkeys to compare the kinematics of stimulation-evoked movements and natural gaze shifts. First, we examined the amplitude–velocity relationship or main sequence during natural gaze shifts as well as during coordinated eye–head movements evoked by electrical stimulation (Freedman et al. 1996; Knight and Fuchs 2007; Martinez-Trujillo et al. 2003b). Second, the relative contributions of the Eh and Hs movements to gaze amplitude: during natural gaze shifts or evoked movements were also analyzed (Freedman et al. 1996; Knight and Fuchs 2007; Martinez-Trujillo et al. 2003a). Since these first two issues have been examined previously in other labs (Chen 2006; Elsley et al. 2007; Knight and Fuchs 2007), they will be treated with brevity here, providing only enough detail for comparison with previous studies and lay the foundation for the next, more novel question. Finally, we determined whether FEF stimulation-evoked movements had 3D kinematics comparable to that of natural behavior, as described earlier. To the best of our knowledge this is the first time the 3D kinematics of FEF-evoked movements have been analyzed in this fashion.

To conclude that electrical stimulation of the FEF results in normally coordinated gaze shifts, one must show that the resulting eye and head movements follow the kinematic profiles described earlier. We found that FEF stimulation elicited combined movements of the eyes and the head that closely resembled naturally occurring gaze shifts in: *1*) the relative contributions of the eyes and head contributions to gaze amplitude, *2*) the velocity–amplitude profiles, and *3*) the 3D constraints (Donders' law and Listing's law). One interpretation of these results is that the FEF encodes gaze and that the details of eye–head coordination are specified downstream from this area.

METHODS

Preparation of the animals

The surgical and experimental procedures used in this study were done in accordance with Canadian Council on Animal Care guidelines and were preapproved by the York University Animal Care Committee. Two female rhesus monkeys (*Macaca mulatta*) weighting 5.3 kg (M1) and 6.5 kg (M2), respectively, underwent surgical procedures

under general anesthesia using 1.5% isoflurane and ketamine 10 mg/kg. During the procedures, each monkey was implanted with a head post, a plastic recording chamber (Narishige Intl. USA Inc., NY), sockets for a cable connection, and two eye coils. Implants were attached to the skull using a dental acrylic cap. The recording chambers were 20 mm in diameter. We implanted one chamber over the right arcuate sulcus in M1 and two chambers in M2, one over the right and one over the left arcuate sulcus (Robinson and Fuchs 1969). The stereotaxic coordinates were 22 mm anterior and 18–20 mm lateral. A craniotomy of the frontal bone (20 mm diameter), which covered the base of the chamber, allowed access to the left or right FEFs. The head post, positioned over the parietal bone and on the midline, consisted of a stainless steel cylinder with a rapid release mechanism (described by Crawford et al. 1999). The two scleral search coils (copper wire of 5-mm diameter) were implanted subconjunctivally (in the nasal half on one eye). These coils were later used to measure 3D eye orientations during training and experimental procedures (for details, see Crawford and Vilis 1991; Tweed et al. 1990). Following the surgery, the monkeys were allowed to recover for 2 wk before training or experiments commenced.

During the training and experiments, each animal wore a primate jacket and was sitting upright in a modified primate chair (Crist Instruments, Hagerstown, MD). The primate chair modifications constrained the animals' torso movements, thus allowing for a larger range of head movements (for details see Constantin et al. 2004). The monkeys were able to make natural and unrestricted movements of the eyes and head, except for gaze directions >50° downward. The chair was placed near the center (±15 cm) of three orthogonal magnetic fields (Tweed et al. 1990). The animals' acrylic skull cap was fitted with two orthogonal coils (1-cm diameter), which allowed measurements of 3D Hs orientations. The eyes and head coil signals were recorded at a sampling frequency of 1,000 Hz. The timing and dose of the water (or fruit juice) reward was controlled by a solenoid valve that delivered the liquid to the animal's mouth by means of a metal pipe. The metal pipe was fixed to the left or right side of the primate chair by means of a plastic clamp secured to the chair.

Training and experimental procedures

SETUP. Animals sat in front of a hemispherical (tangent) screen with a radius of 100 cm and were trained to make visual gaze shifts in the dark toward light-emitting diodes (LEDs); the LEDs were fixed to the back of the screen at various eccentricities and the animals were trained to make head-unrestrained gaze shifts to the LEDs. The experimental room was dark except for the LED emission. Eight LEDs in the array were positioned at 20° viewing distance from a central LED, in radial directions of 0, 45, 90, 135, 180, 225, 270, and 315°. In such an arrangement, the LED at 0 was in the horizontal plane and rightward from the eyes of the monkey and the LED at 90° was in the vertical plane and upward relative to the eyes of the monkey. Another set of eight LEDs were positioned in the same radial directions as the previous round of LEDs but at 40° viewing distance from the central LED.

BEHAVIORAL TASK. Each animal was trained to make visually guided gaze shifts to a step change in target position between two sequentially illuminated LEDs from our LED array. Animals were allowed to select natural patterns of eye–head coordination. LEDs were illuminated pseudorandomly to reduce the predictability of the size and direction of the target step. LEDs were illuminated for 300 or 500 ms, accompanied by a brief auditory tone originating at the same general location of the active LED. This tone was used as an auxiliary indication for the animal to make an orienting movement (we have found that this helps animals to attend to more peripheral targets). Animals were required to direct gaze toward the LED within a spatial window with radius 5 to 8° from the LED. After each successfully completed trial the animal received a drop of fruit juice or water as a reward.

In some sessions, in which the animals were not motivated to work for the liquid reward, the monkeys were simply allowed to move their eyes and heads freely and naturally. Some of these movements were self-initiated, whereas others were encouraged as follows. During these sessions one experimenter stood hidden behind a hemispherical dome [barrier paradigm (Guitton et al. 1990; Klier et al. 2003)] and motivated the monkeys to use their entire eye–head motor ranges by presenting the monkeys novel visual objects (in dim light) and novel sounds (in the dark). A second experimenter viewed the eye–head movements on-line and provided verbal feedback about the range of initial positions obtained. This was done to obtain the large range of initial eye and head positions necessary for our analysis.

We did not systematically train the animals to dissociate the relative pointing directions of the eyes and the head during gaze fixations. Animals were free to choose any desired combination of eye–head positions when fixating the targets. This avoided eye–head coordination patterns driven by specific contexts, which can affect the kinematics of natural and electrically evoked eye–head movements (Monteon et al. 2007; Oommen et al. 2004).

Microstimulation procedures

Electrophysiology experiments began after an approximate training period of 3 wk, in each monkey. Stimulation was generated by a stimulator and one constant-current stimulus isolation unit (model S88 and PSIU-6; Grass Instruments) and delivered through a tungsten microelectrode (0.8–1.2 mΩ impedance at 1 kHz; FHC). We monitored the current to be delivered to the electrode by examining the output of the isolation unit. This was done by monitoring the waveshape amplitude of the voltage proportional to the current in an oscilloscope (Hung Chang 5504). The electrode was lowered by a low-weight (48 g) hydraulic microdrive customized for head-unrestrained experiments (Narishige). During each experiment we made penetrations at one or two locations (tracks) with a maximum vertical excursion of the electrode of 10 mm. We then applied a standard stimulation train (0.5 ms/pulse, 300-Hz frequency, 200-ms duration, cathodal pulse). Initially, the head was restrained while we searched for a site that could evoke saccadic eye movements at low current thresholds (<50 μA intensity). After finding a low-threshold site, we released the animal's head and delivered higher currents aimed at evoking eye and head movements (Chen 2006; Knight and Fuchs 2007; Tu and Keating 2000) (60–100 μA, typically 80 μA). Given such low thresholds, and the timing and metrics of the evoked movements presented in RESULTS, we are confident that stimulation was delivered to the low-threshold region of the FEF (Bruce et al. 1985).

In the case of the stimulation experiments, stimulation trials were intermixed randomly with normal, visually guided gaze shifts at a ratio of about 1:3. Each stimulation trial began at a fixated LED position that was randomly varied across trials to elicit different initial eye and head positions. After the animal fixated the target for 300 or 500 ms, the LED was extinguished and a stimulation train was delivered after pseudorandom delays within 50–300 ms after fixation target offset. No visual stimulus was present during the electrical stimulation trains. In stimulation trials animals received a water or juice reward 100–200 ms after the stimulation offset, independently of gaze position. In some sessions when the animal was not motivated to obtain the water reward we used the above-mentioned barrier paradigm (Guitton et al. 1990; Klier et al. 2003). In this case the stimulation trains were delivered at a variety of initial eye and head positions that were self-initiated or encouraged (see BEHAVIORAL TASK).

After recording several evoked trajectories corresponding to a given stimulation site we advanced the electrode by 500 μm vertically and repeated the process. For clarity, we refer to a stimulation site as

a unique stimulation location within the FEF. As in previous reports we arbitrarily considered different stimulation sites to be locations separated by a minimum of 500 μm (Chen 2006; Elsley et al. 2007). Movements obtained from each site were pooled and analyzed independently from the other sites. In 11 sites from M1 and 13 sites from M2 (that consistently evoked gaze movements $>10°$) we applied a series of 10–30 stimulations at each of four different stimulation durations: 100, 300, 400, and 500 ms. Note that the fifth stimulation duration corresponded to our standard stimulation train of 200-ms duration (recorded in all the explored sites); in this case we typically delivered nearly 40 stimulation trains (median 39) per site at random LED locations.

Data analysis

From the raw coil signals we computed quaternions to represent the orientation of the Es and Hs with respect to the reference position (Tweed et al. 1990). The quaternions were expressed in a right-hand coordinate system aligned with the coils. The orientations of the Eh were computed by inverting the Es quaternions and multiplying them by the correspondent Hs quaternions (Glenn and Vilis 1992). All the quaternions (Es, Hs, and Eh) were converted not only into 3D vectors scaled by their angle of rotation (Crawford and Guitton 1997) but also into angular velocity vectors for the off-line analysis. From the position quaternions, 2D gaze trajectories were also obtained (Tweed et al. 1990). For the Es, these trajectories describe changes in the line of sight as if one were observing the animal from behind and its fovea was projecting a spot of light onto a hemisphere centered on the eye (see Fig. 2). Angular Es, Hs, and Eh velocities were calculated for each stimulation-evoked movement. These were then averaged across all the movements for a given site and plotted as a function of time from the stimulation onset.

Stimulation-evoked movements were included in the analysis if their gaze peak velocity was $>50°$/s and the latency from stimulation onset to gaze peak velocity was >10 ms and <200 ms. The exceptions were the sites that coded for gaze shifts with amplitudes $\geq 70°$; in this case we allowed a latency from stimulation onset to gaze peak velocity of >10 ms and <250 ms. Only the first evoked gaze shift was analyzed; we did not include sites that coded multistep gaze shifts in $>50\%$ of the stimulation-evoked trials. Also, individual trials with multistep gaze shifts were excluded from the analysis (sites that did not meet the criteria were discarded). From 129 sites, 95 sites met the inclusion criteria (52 in M1, 43 in M2). For the included sites, the quaternions were plotted as a function of time and those representing eye positions at the beginning and end of each stimulation-evoked gaze shift were manually selected by an experienced observer (Constantin et al. 2009; Martinez-Trujillo et al. 2003b). A set of natural gaze shifts were selected during each recording sessions to be used as a control for the stimulation data. These natural movements were intermixed with the stimulation trials and were selected in such a way that for every Es initial and final position of the stimulation-evoked movements, there was at least one comparable natural movement with similar Es initial and final positions (see details in the following text). This procedure guaranteed that the two movement samples were similar enough that the movements' kinematics could be reasonably compared.

The 3D position vectors from the stimulus-evoked selected signals were used to compute the amplitude of each gaze shift as well as the characteristic vector (CV) for Es, Hs, and Eh at each stimulation site. The CV was computed through a multiple linear regression procedure performed on the stimulus-induced movement displacement as a function of initial vertical or horizontal position (Klier et al. 2001). The CV describes the theoretical gaze, eye, or head trajectory that would be elicited if stimulating with the eyes and head pointing straight ahead. This method has the advantage of being robust to variations in the spatial distribution of initial eye positions. For the CV analysis we included data only from sites at which we evoked at least seven movements from different initial gaze positions, which were evenly dispersed around the center, and that covered at least three of the four spatial quadrants. It has been well established that the kinematics of Es, Hs, and Eh movements depend on their initial position. This is the case for both behavioral movements (Delreux et al. 1991; Freedman and Sparks 1997; Tomlinson 1990; Tomlinson and Bahra 1986; Volle and Guitton 1993) and FEF stimulation-evoked movements (Chen 2006; Knight and Fuchs 2007; Tu and Keating 2000).

To avoid any effect of the initial Es and Hs positions on stimulation-evoked movements, we compared them against naturally occurring movements with similar initial position range for both Es and Hs. In our statistical analysis, we paired each stimulation-evoked movement with a corresponding naturally occurring movement that had the closest initial gaze and head position.

The closest position was automatically selected by a computer algorithm that choose the natural movement within a maximum range of 8° for the Es and 16° for the Hs from the corresponding stimulation-evoked initial Es and Hs positions. Once a movement was selected, it was excluded from the pool. This method was used for analysis of the relative contributions of the eyes and the head to gaze movements' amplitude and the amplitude–velocity profiles (Supplemental Figs. S4 and S5, respectively).[1] The comparisons between naturally occurring movements were done using a series of statistical tests including: ANOVA for the velocity–amplitude profiles and the relative contributions of the eyes and the head to gaze; sign test for comparison of the characteristic vectors; Student's *t*-test and/or bootstrapping methods for the 3D kinematics. For the bootstrapping analysis we first fit the response torsional amplitude for the saccadic and VOR phases to each condition (naturally occurring and stimulation-evoked movements) with a line using a least-squares algorithm. We then tested whether the slopes (or differences between slopes) were significantly different from zero using bootstrapping; we resampled the data with replacement 10,000 times, fit each resampled data set with a line; and calculated the 95% confidence intervals on the resulting distributions of bootstrapped slopes. In subsequent sections all the values corresponding to descriptive statistics will state the mean ± SD unless otherwise noted.

3D analysis

To determine how well the stimulation-evoked movements followed the 3D constraints described for natural gaze shifts in the monkey, we quantified the 3D range of orientations for the Es, Hs, and Eh: first, during periods of normal fixations (Es $\leq 20°$/s and Hs velocities $\leq 10°$/s) and, second, at the end of the stimulation-evoked head movements. Similar methodologies have been used in previous 3D studies in macaques (Crawford et al. 1999; Martinez-Trujillo et al. 2003b). This was done by determining the second-order surfaces of best fit to the Es, Hs, and Eh position quaternions (Crawford et al. 1999; Glenn and Vilis 1992; Misslisch et al. 1998; Radau et al. 1994; Tweed and Vilis 1990; Tweed et al. 1990). The second-order surface is described by the equation $q_1 = a_1 + a_2q_2 + a_3q_3 + a_4(q_2)^2 + a_5q_2q_3 + a_6(q_3)^2$, which expresses torsional position (q_1) as a function of vertical (q_2) and horizontal (q_3) position. This equation is an analog in a 3D space of a linear regression model in a 2D space. For both data sets (fixation points and end of stimulation-evoked head movements), we computed the torsional variability or torsional SDs. This measurement indicates how closely the orientations of Es, Hs, and Eh cluster around their surfaces. The smaller the torsional SD, the more the quaternions adhere to their surface (Crawford et al. 1999; Tweed et al. 1990).

[1] The online version of this article contains supplemental data.

Anatomical location of recording sites

A postmortem histological verification of electrolytic lesions within the stimulation chamber area confirmed that all the stimulation sites reported in this study were located within the arcuate sulcus or surrounding areas. Anatomical reconstructions of the stimulation sites were made. For this purpose, the position of the recording chamber borders relative to the brain surface was determined and high-resolution digital images were taken of the entire brain from different views. The reconstruction of the penetration sites was made by superimposing a digital grid onto the chamber location. The x- and y-coordinates of each penetration site were prelocated within the grid and then remapped onto the brain surface (Fig. 1, *A* and *C*). In addition, a 3D map of the recording chamber was reconstructed (Fig. 1, *B* and *D*). The coordinate axis of this 3D map consisted of the anteroposterior coordinates (*x*-axis), the mediolateral coordinates (*y*-axis), and the dorsoventral coordinate (*z*-axis). The locations of the electrode tips at the time of the cortical penetration were superimposed onto this map. Figure 1*B* shows the location of the 52 FEF sites (circles) for M1 and 43 FEF sites for M2 (Fig. 1*D*). The data and conclusions in the following sections apply only to the sites of the prefrontal cortex indicated in Fig. 1. Each of these sites met the inclusion criteria described in *Data analysis*.

RESULTS

After a thorough exploration of the recording chambers via our electrode probes, we identified (on-line) 129 FEF sites in the two animals (70 in M1; 59 in M2) where stimulation evoked gaze shifts. In an off-line analysis, we found that stimulation of 95 sites, 52 in M1 and 43 in M2 (Fig. 1), consistently evoked Hs and Eh movements with regular latencies and velocity profiles (see METHODS). The subsequent sections present our analysis of these 95 sites. Unless stated otherwise, standard 200-ms trains were used.

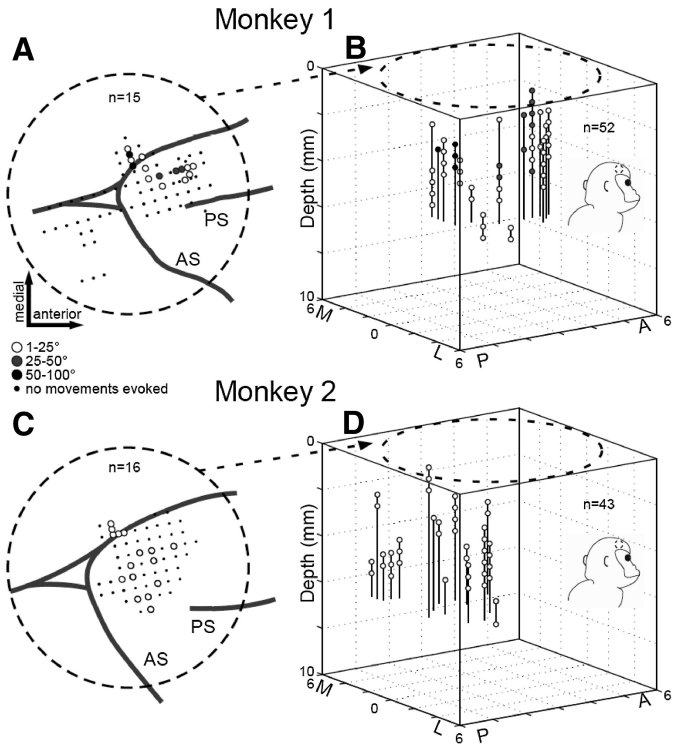

FIG. 1. Anatomical reconstruction of stimulation sites. *A* and *C*: *top view* of the anatomical reconstruction of the right frontal cortex in M1 (*A*) and M2 (*C*); dashed lines represent the diameter and position of the recording chamber. Dots represent the site of the electrode penetration according to their characteristic vector (CV) amplitude (see METHODS: *Data analysis* and Fig. 3). AS, arcuate sulcus; PS, principal sulcus. *B* and *D*: 3D reconstructed map with the locations of the stimulated sites (black circle), with a total of 52 stimulation sites from M1 (*B*) and 43 sites for M2 (*D*). The monkey head caricature allows for a better orientation of the cube position.

Stimulation-evoked movement latencies

Movement latencies were defined as the time from stimulus onset to movement initiation (Supplemental Fig. S1). The gaze latency (mean in ms ± SD) values were shorter than head latency values for both monkeys. The mean latency for gaze movements in M1 was 71.05 ± 40.86 ms (median = 61). The mean head latency for gaze movements was 82.64 ± 42.60 ms (median = 73). In the case of the second animal, mean gaze latencies were 66.25 ± 37.54 ms (median = 56). Mean head latencies were 78.96 ± 38.22 ms (median = 69). The mean latencies for gaze and head movement were significantly different for both animals (paired *t*-test with Holm–Bonferroni correction for multiple comparisons, $P < 0.001$).

Amplitude and directions of the evoked movements

To determine the average amplitude of the Es, Hs, and Eh movements across different sites, we obtained 2D trajectories for all the stimulation-evoked movements for each one of the sites. Figure 2 shows examples of trajectories evoked by stimulating two sites (*left* and *right columns*) in the right FEF in M1. The *top three rows* of the figure show behind views of Es, Eh, and Hs trajectories, respectively, during the gaze-shift phase of the movements. The *bottom row* shows the complete head movement. The lines represent the trajectories and the circles their endpoints. For both sites the Es, Hs, and Eh movements were in the same direction and contralateral to the stimulated site. These data show that both the Hs and Eh contribute to the Es movements.

To quantitatively corroborate this, we quantified the amplitude of the movements across the different sites by computing the movements' characteristic vector (CV; see METHODS). The arrows in Fig. 2 show the CV values of the stimulation-evoked trajectories for Es, Eh, Hs (end of gaze shift), and Hs (complete movement). The CV is pointing upward and to the left, like many of the individual trajectories. Note that individual trajectories could be larger or smaller that the CV because the latter approximates an average across the population. Figure 3, *A–C* shows a behind view of the spatial distribution of the CV values for the Es in M1 (*A*, *B*) and M2 (*C*). Their distribution spans both sides of the horizontal line meridian, with the majority of the CV values having a marked oblique component. Without exception, the CV of each site is contralateral relative to the stimulated brain hemisphere. This arrangement corroborates the results of previous stimulation studies (Bruce et al. 1985; Chen 2006; Elsley et al. 2007; Knight and Fuchs 2007; Tu and Keating 2000).

The mean CV for the eye-in-space was 23 ± 16° for all the sites in M1. However, they were four sites that coded very large evoked movements (Fig. 3*B*). When excluding these sites, the eye-in-space mean CV was 19 ± 7°. The mean CV for the Es of the four sites with large evoked movements was 70 ± 24°. We report the mean CVs for these sites separately (see Fig. 3, *left* and *middle columns*) so that they can be distinguished from more typical sites in our population. For M2 the mean CV for Es was

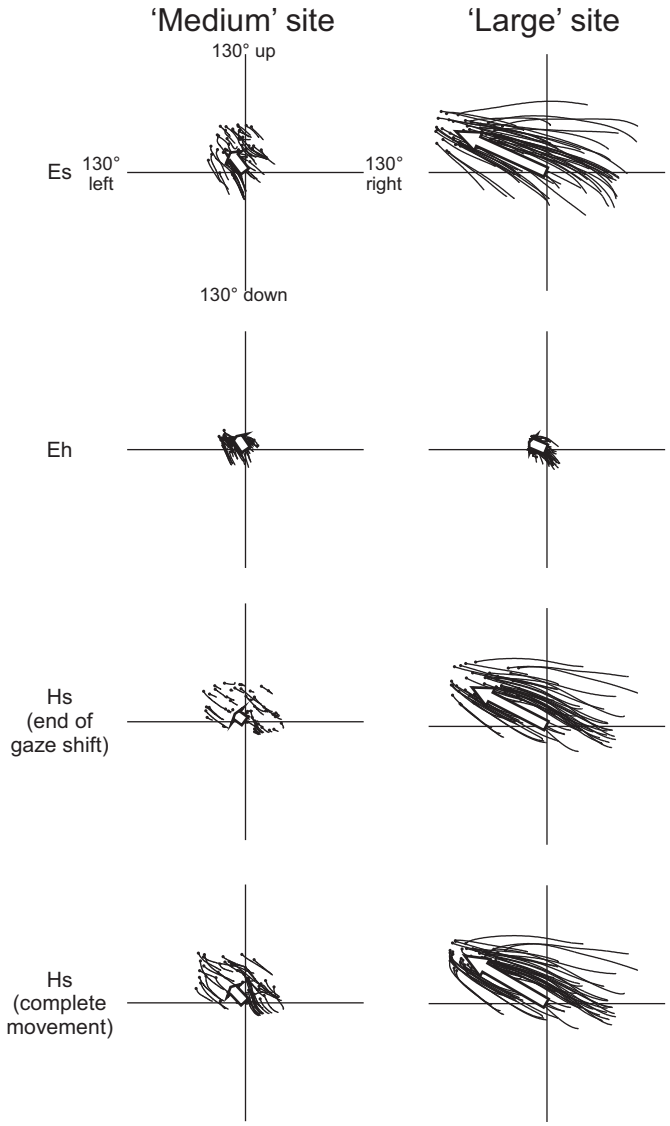

FIG. 2. Examples of stimulation-evoked movement trajectories. Behind view of trajectories evoked by stimulating 2 frontal eye field (FEF) sites on the right hemisphere of monkey 1. The abscissa represents the horizontal meridian and the ordinate, the vertical. The lines represent the trajectories, their free extreme represents the initial position, and the circles represent the final position at the end of the gaze shift phase. *Top*: movements of the eyes-relative-to-space (Es) data; *middle top*: movements of the eyes-relative-to-head (Eh) data; *middle bottom*: movements of the head-relative-to-space (Hs) data. *Bottom*: Hs trajectories ending at the end of the vestibuloocular reflex (VOR) phase (complete movement). Arrows show the CV of each movement component for that site. Data collected from M1.

10 ± 5°. In the case of the CVs for the Eh (Fig. 3, *D–F*) the mean CVs were: 13 ± 6° for all sites in M1 and 13 ± 6° when the sites with large evoked movements were excluded (mean for large sites: 13 ± 1°). For M2 the mean CV was 9 ± 4°. The mean Hs CVs were: 13 ± 17° for all sites in M1 and 9 ± 5° when the large sites were excluded (mean for large sites: 65 ± 23°). For M2 the mean CV was 4 ± 4°.

Comparison between stimulus-evoked movements and natural gaze shifts

To test whether the stimulation-evoked movements have similar kinematics to that of natural gaze shifts, we recorded both: trials of natural gaze shifts made by the animals and trials in which the stimulations were delivered, in which these two types of trials were randomly intermingled. All movements were classified according to their amplitude and then pooled within each sample for quantitative comparisons of kinematics between the two samples. It is well documented that kinematics of movements of Es, Eh, and Hs depend on their respective initial positions for both FEF stimulation-evoked movements (Chen 2006; Knight and Fuchs 2007; Tu and Keating 2000) and natural gaze shifts (Delreux et al. 1991; Freedman and Sparks 1997; Tomlinson 1990; Tomlinson and Bahra 1986a; Volle and Guitton 1993). To control for such initial position dependence we compared stimulation-evoked and natural gaze shifts that had a similar range of initial positions. We paired each stimulation-evoked movement with the natural movement that had the closest initial Es and Hs positions (see METHODS).

Eye–head contribution

An aspect of kinematics of movements that characterizes natural gaze shifts is the relationship between the relative contributions of the Hs and Eh to Es movement amplitude. We assessed whether the stimulation-evoked movements were similar to natural gaze shifts in this aspect. For each monkey, we divided gaze shifts into five bins of width 10°. Then we obtained the mean amplitudes of the corresponding Hs and Eh movements. These produced a total of 20 pairs of mean values for statistical comparison. Of these only 4 showed a statistically significant difference between stimulation-evoked versus natural gaze shifts. (For full details of this analysis see Supplemental Fig. S4 and related text.) Based on these findings we concluded that microstimulation of the FEF evoked gaze shifts with normal eye and head contributions, as observed previously (Knight and Fuchs 2007).

Velocity–amplitude profiles

For natural gaze shifts in the head-free macaque, the peak velocities of the Es, Hs, and Eh vary stereotypically as a function of gaze amplitude (the main sequence). We assessed whether the stimulation-evoked movements showed a similar variation by comparing the curves relating these two variables between the samples of stimulation-evoked and natural gaze shifts. In general this analysis showed that the kinematics of stimulation-evoked and natural movements were very similar, but not the same. For most Es amplitudes (21 of 30 pairs of mean values) there was no difference between stimulation and natural movements. For full details of this analysis see Supplemental Fig. S5 and related text.

3D kinematics

During natural fixations, the eyes and the head approximate Donders' law (Donders 1848), which states that for any one 2D (vertical and horizontal) gaze pointing direction, there is a unique and constant amount of torsional rotation. These 3D constraints have been shown to be obeyed most closely during fixations at *1*) the end of the VOR phase of natural gaze shifts in monkeys (Crawford and Vilis 1991; Crawford et al. 1999) and *2*) the end of the similar phase of gaze shifts evoked by stimulating the SC (Klier et al. 2003) and the SEF (Martinez-Trujillo et al. 2003b) but not the lateral intraparietal cortex

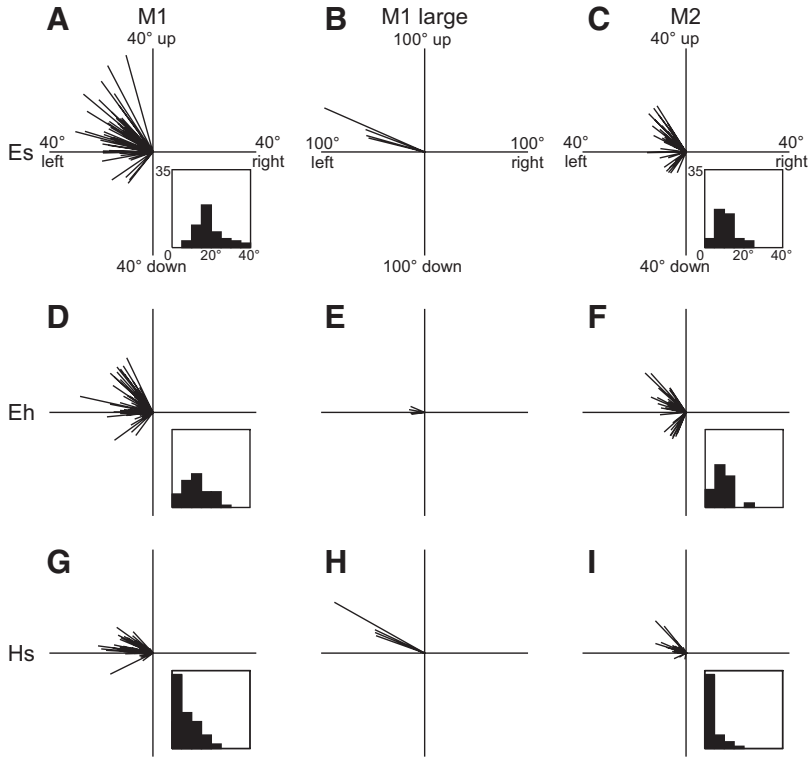

FIG. 3. Spatial distributions of the CV. Behind view of the spatial distributions of the CVs in all the stimulation sites for the Es (*top row*), Eh (*middle row*), and Hs (*bottom row*). CVs for M1 were divided into large CVs (>50°, *middle column*) or typical CVs (*left column*). Data for M2 are presented on the *right column*. The *inset* in the plots represents the distribution of CVs for the corresponding condition. In the histograms, the abscissa represents the amplitude of the CVs and the ordinate, the number of sites.

(Constantin et al. 2009) or the interstitial nucleus of Cajal (INC) (Farshadmanesh et al. 2008; Klier et al. 2007). Moreover, it has been shown that this can occur only if the eyes and head are very precisely coordinated. Here we similarly assessed whether the same constraints are obeyed at the end of movements evoked by stimulating the FEF. First, we computed 3D position quaternions for the Es, Hs, and Eh during natural fixations and, second, we fitted 3D surfaces to them (see METHODS).

Figure 4 shows data from one example experiment in animal M1. The graphs (*A–F*) display the horizontal components (ordinate) of the axis of rotations (quaternions converted to angles) for the Es (*A*, *D*), Hs (*B*, *E*), and Eh (*C*, *F*) as a function of the torsional components (abscissa) plotted in right-hand rule coordinates. For example, a data point falling in the left upper quadrant represents a counterclockwise and leftward movement. The planes represent the Donders' surfaces (2D range given by the best polynomial fit through the data; Constantin et al. 2009). Observe that the forward vertical and horizontal edge of the surfaces has been highlighted (black thick line) to facilitate visual interpretation of these 3D plots. The *left column* of Fig. 4, *A–C* shows an example corresponding to data points from naturally occurring fixations. It can be seen that, as the positions depart from the center, the Es (*A*) and Hs (*B*) surfaces show larger deviations from the ordinate than the Eh surface (*C*), corroborating that for the Es and Hs Donders' law is obeyed but not Listing's law (Crawford et al. 1999). In contrast, the Eh falls within a flat surface similar to the Listing's plane observed with the head fixed (Tweed and Vilis 1990). Figure 4, *middle column* (*D–F*), displays the same surfaces as on the *left* (fit to the behavioral data), but with the data corresponding to the end of the stimulation-evoked movements plotted on the surfaces. These stimulation data seem to adhere quite well to the surfaces, suggesting that at the end of the stimulation-evoked movements Donders' law and Listing's law are also obeyed.

However, the space-fixed coordinate system we have used to plot the data in Fig. 4, *A–F* does not allow one to visualize the relatively tight 3D control of Es, Hs, and Eh positions relative to the curved and twisted Donders' surfaces. This is better seen by plotting the stimulation-evoked data in a new coordinate system (Donders' coordinates) where the vertical and horizontal axis are aligned with the Donders' surface and the torsional axis represents deviations from the Donders' surface. Figure 4, *G–I* displays stimulation endpoints for the Es (*top*), Hs (*middle*), and Eh (*bottom*) for the same stimulation example shown in Fig. 4, *D–F* in Donders' coordinates. Observe that in this new coordinate system the abscissa represents the deviation of the data from the surface and the ordinate, the surface. In all cases, the data are closely distributed at both sides of the ordinate, reflecting that they adhere well to their corresponding surfaces. In both examples, there is more spread along the horizontal axis for the Es, followed by the Hs, and much less for the Eh, reflecting a tighter control of the torsional component of the movement for the Eh relative to the Hs and Es. To quantify this spread, we determined the mean deviation of the data from the point of zero torsion, in this case from the ordinate. This measurement, known as torsional SD, has already been used in previous studies of 3D gaze kinematics (Crawford et al. 1999; Glenn and Vilis 1992; Klier et al. 2003; Radau et al. 1994).

The M1 natural fixation example in Fig. 4 has torsional SDs of 5.20, 4.73, and 2.13° for the Es, Hs, and Eh, respectively. The stimulations-evoked example, from the same recording session, has torsional SDs of 5.04, 4.75, and 1.56° for the Es, Hs, and Eh, respectively. These suggest a similar torsional control in natural and stimulation-evoked movements. The only exception to this rule was a single site (Supplemental Fig.

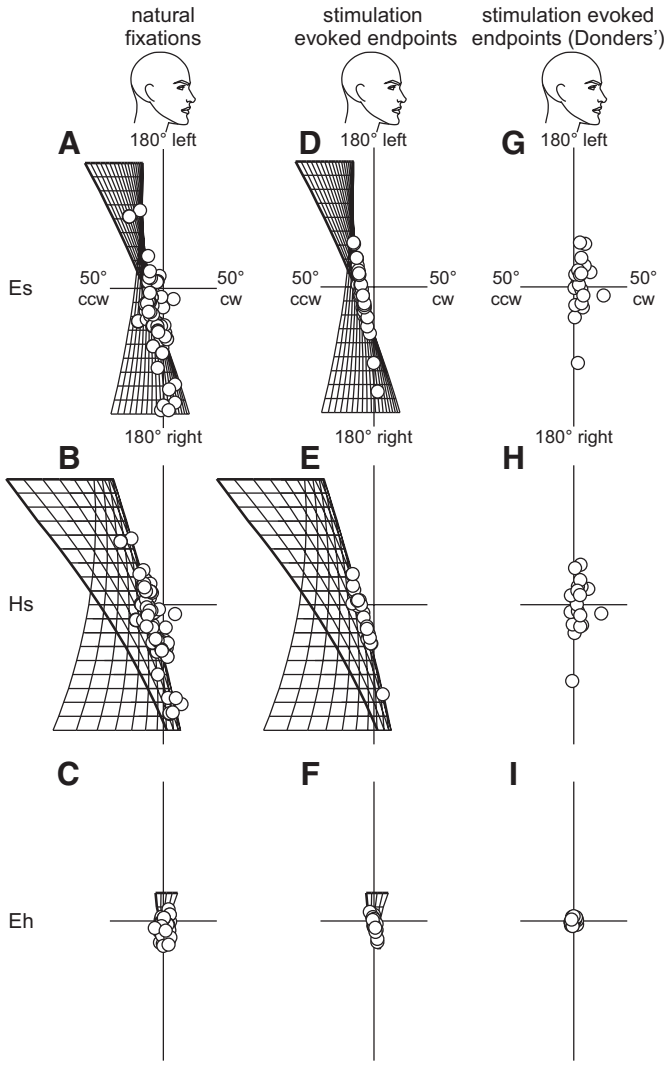

FIG. 4. Three-dimensional (3D) analysis for one stimulation site. *A–F*: scatterplots of the torsional (abscissa) and horizontal (ordinate) components of Es (*top*), Hs (*middle*), and Eh (*bottom*) position quaternions converted to angles of rotation in right-hand rule coordinates. 3D surfaces fitted to the data points are represented. *Left* (*A–C*): natural fixations; *middle* (*D–F*): stimulation endpoints. *G–I*: scatterplots of the stimulation endpoints quaternions torsional components (abscissa) against the horizontal components (ordinate) in Donders' coordinates. *Top*: Es; *middle top*: Hs; *middle bottom*: Eh data.

S6 and accompanying text, not included in the present analysis). This site produced large torsional head movements, but unfortunately the eye coils were not functioning that day so we could not establish whether that was a gaze control site. This analysis was done for each stimulation site. As a control the torsional SDs of the natural fixation data were also calculated.

Figure 5 summarizes the results of this analysis for the two animals. It shows the average torsional SDs across sites for the natural fixations (Fig. 5, *A* and *C*) and for the stimulation-evoked movements (Fig. 5, *B* and *D*). In each case, the Es and Hs average torsional SDs were significantly larger than those for the Eh ($P < 0.001$, paired *t*-test). The average values for natural movements in M1 were 7.14 ± 3.21, 7.64 ± 4.58, and 2.67 ± 3.47°, for Es, Hs, and Eh, respectively. For stimulation-evoked movements in M1 the values were 7.08 ± 4.06, 7.17 ± 3.87, and 2.09 ± 1.42° for Es, Hs, and Eh. In the case of M2, the average values for natural movements were 3.79 ± 1.64, 3.85 ± 1.60, and 1.84 ± 1.16° for Es, Hs, and Eh. The values corresponding to stimulation-evoked movements were 3.42 ± 0.94, 4.44 ± 1.23, and 1.85 ± 0.69°. For the two animals, we found no significant differences between natural fixations and stimulation-evoked endpoints ($P < 0.05$, paired *t*-test). In summary, our analysis has shown that stimulation-evoked movements follow the same 3D constraints as those of natural fixations.

Another key aspect of torsional control during natural behavior in the gaze control system is that during a gaze shift the Eh torsion is first driven out of Listing's plane such that the following VOR-related head movement brings the Eh back into Listing's plane at the end of the head movement. This strategy has been shown in both humans (Tweed et al. 1998) and monkeys (Crawford et al. 1999). In contrast, when the head is motionless, the Listing's law is obeyed and the Eh always has near zero torsion (Ferman et al. 1987a; Tweed and Vilis 1990). We asked the question of whether the FEF stimulation-evoked movements obey this kinematic rule. We compared head-restrained and head-unrestrained gaze shifts naturally occurring against those evoked by stimulation in the same conditions.

Figure 6, *A–C* shows examples of natural behavior, with eye torsion plotted in Listing's coordinates. Figure 6*A* plots torsional eye position as a function of time for a typical head-free saccade (solid line) and a typical head-fixed saccade (dotted line). The head-fixed saccade essentially remained in Listing's plane (near zero), whereas the head-free saccade had a fast torsional component that was followed by a slower torsional VOR phase in the opposite direction. The same pattern can be

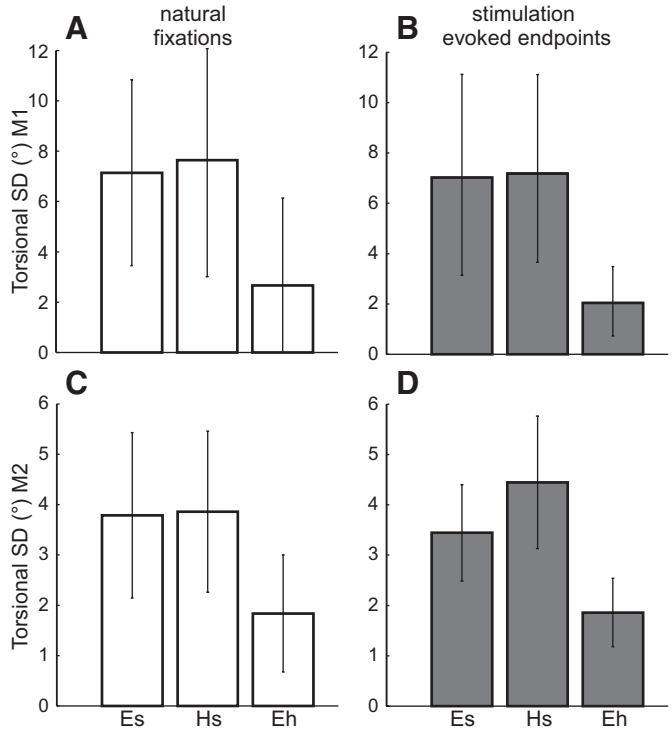

FIG. 5. Average torsional SDs. Average torsional SDs during natural fixations (*A*, *C*) and stimulation endpoints (*B*, *D*). The abscissa displays Es and its 2 components (Hs and Eh) and the ordinate displays the average torsional SD in degrees. *Top*: data from M1; *bottom*: data from M2. The error bars represents SDs.

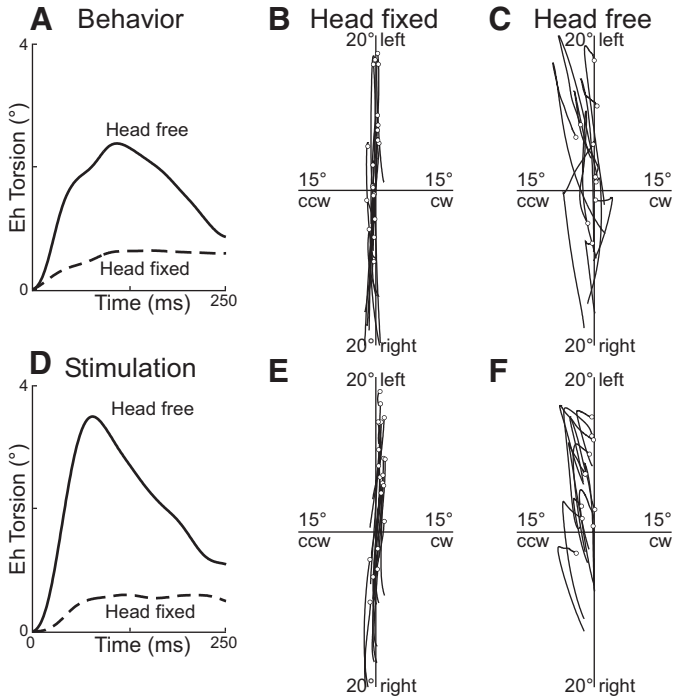

FIG. 6. Torsion during saccadic and VOR phases. *A* and *D*: eye torsion trajectories during head-fixed (dashed lines) vs. head-free (filled line) movements, are plotted as a function of time in Listing's coordinates; the movement traces are aligned on initial position and beginning of stimulation. 2D plot of the torsional (abscissa) and horizontal (ordinate) components of eye position quaternions converted to angles of rotation in right-hand rule coordinates, plotted in Listing's plane. *B*, *C*, *E*, and *F*: scatterplots of the torsional Eh movements in Listing's coordinates (abscissa) vs. the horizontal Eh component (ordinate), with the head fixed (*B* and *E*), torsion remains in Listing's plane (i.e., parallel to the plane of 0 torsion) throughout behavior (*B*) and stimulation-evoked (*E*) movements. With the head free (*C* and *F*), torsion is driven out of and then back into Listing's plane during behavior (*C*), as well as stimulation (*F*); ○ shows the end of the movement. Movements were matched for size and initial position.

seen in the 2D (torsional vs. horizontal Eh components) trajectories in a series of head-fixed saccades (Fig. 6*B*) and head-free saccades (that include the VOR phase) (Fig. 6*C*). As mentioned earlier, these observations were previously reported.

Figure 6, *D–F* shows similar plots as in the previous case but for stimulation-evoked movements. With the head fixed (Fig 6, *D* and *E*) Listing's law of the Eh is also obeyed because the torsional values remain near zero. However, for the head free, during the saccadic phase of the movement the torsional component was brought out of Listing's plane and then back to the plane during the VOR phase. These examples suggest that the natural and stimulation-evoked movements have comparable kinematics during the saccadic phase and VOR phase of the movements.

To quantify these visual observations we plotted torsional values during the saccadic and VOR phases. Figure 7*A* shows scatterplots of average absolute torsion for head-unrestrained versus head-restrained saccades for 33 stimulation sites in which we collected both data sets. The head-unrestrained torsional Eh mean amplitude (1.89 ± 1.34°) was significantly larger that the head-restrained torsional Eh mean amplitude (0.75 ± 0.24°) ($P < 0.001$, Sign test).

Figure 7, *B* and *C* plots the values of the VOR torsional component as a function of the torsional component of head-unrestrained saccades from M1 and M2, respectively. Stimulation-evoked movements are shown, along with a similar population of behavioral data. In the behavioral data, the saccade amplitude and VOR torsion were correlated. In M1 the correlation coefficients were −0.52 and −0.34 and the slope values were −0.37 and −0.18, for natural and stimulation-evoked movements, respectively. For M2 the coefficients were −0.49 and −0.47 and the slope values were −0.29 and −0.29. We used bootstrapping methods to test for differences between the slopes of naturally occurring and stimulation-evoked movements. For M1 the difference between the slopes of natural and stimulation movements were statistically different from zero. The corresponding data for M2 showed no statistical difference from zero.

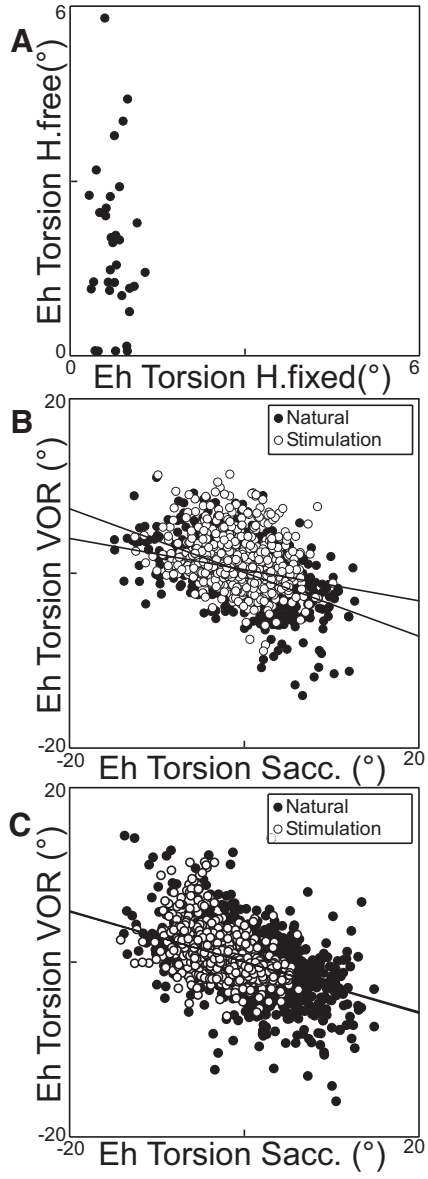

FIG. 7. Torsion during saccadic and VOR phases: population effects. *A*: mean absolute torsion for head-fixed Eh saccade (abscissa) as a function of Eh head-free saccade. *B* and *C*: the torsional Eh saccadic component (abscissa) in relation to the Eh VOR component (ordinate) for M1 (*B*) and M2 (*C*). Symbols display stimulation-evoked (○) and natural eye movements (●).

The bootstrapping analysis took into account the direction of the Eh torsional movements: clockwise or counterclockwise (negative and positive values, respectively). However, the percentage of counterclockwise movements was greater in stimulation trials than that in behavioral trials (Fig. 7, *B* and *C*, ordinate axis): 47% (M1) and 49% (M2) of the movements during the Eh saccade were counterclockwise during the behavioral experiment. The corresponding values for the stimulation experiment were 63% (M1) and 64% (M2). Due to this directional bias in stimulation trials we repeated our bootstrapping analysis using absolute torsional values. We found no statistical difference from zero between the difference between slopes of stimulation-evoked and natural movements for M1 or M2. In summary, our analysis has shown that during the saccadic and VOR phases, the stimulation-evoked movements possess the same 3D constraints as those of natural movements. This corroborates that the evoked movements were indistinguishable from natural gaze shifts.

DISCUSSION

The present study attempted to determine the nature of the motor output of the FEF. We found that in 95 sites electrical stimulation (see METHODS) evoked Es movements with regular and consistent latencies. Such movements were a combination of Hs and Eh rotations. Their 2D and 3D kinematics (velocity–amplitude relationship, relative contributions of the eyes and head to the movements, and compliance with Donders' law) were comparable to the kinematics of natural gaze shifts. Our findings suggest that the relative contribution of the eyes and head to gaze as well as other kinematic aspects of eye–head coordination during gaze shifts are implemented by structures located downstream from the FEF. In addition, our results demonstrate that the motor output of the FEF is a gaze command composed of coordinated Hs and Eh movements. We presented several lines of evidence that support this conclusion.

First, with durations of 200 ms stimulation the majority of sites in the FEF evoked gaze shifts with eye and head movement components (see *Amplitude and directions of the evoked movements* and Fig. 3, *A–I*). In addition, the gaze shifts elicited by 200-ms-stimulus trains resembled those of naturally occurring gaze shifts of the same size. In particular, the relative contributions of the eye and head movements were very similar whether the gaze shift was visually or stimulus evoked (see *Eye–head contribution* and Supplemental Fig. S4). Similarly, the profile of the relationship between the peak velocity and the movement's amplitude (also known as the main sequence) remained similar when comparing the stimulation-evoked movements with their behavioral counterpart (see *Velocity–amplitude profiles* and Supplemental Fig. S5). Three-dimensional motion analysis also supported the view that the FEF-evoked movements mimic natural behavior. For instance, the torsional mean deviation of the data from the point of zero torsion (torsional SD) showed that the naturally occurring movements and stimulation-evoked movements of Es, Hs, and Eh are indistinguishable in this regard. A similar result was obtained when we compared the torsional components of natural and stimulation movements during the saccadic and VOR phases of the Eh trajectories.

These results do not necessarily suggest that natural, physiological patterns of neural and muscular activity were produced by FEF stimulation (e.g., see Elsley et al. 2007). Conversely, it is possible that unnatural patterns of activation, such as activation of fibers en passant or nonphysiological combinations of FEF activity with other brain states, may have contributed to some of the noise to our results (Chen and Tehovnik 2007; Russo and Bruce 1993). However, with regard to the question we asked—whether microstimulation of FEF produces normal 3D patterns of eye–head coordination—the answer appears to be yes.

Comparison with other studies

Our study is in general agreement with studies by Knight and Fuchs (2007), Tu and Keating (2000), and Elsley et al. (2007) who were able to evoke shifts of gaze composed of coordinated movements of the eyes and the head where the head movement onset (relative to stimulation) lagged gaze onset by <30 ms. For instance, Tu and Keating (2000) reported mean latencies of 47.0 and 58.3 ms for Es and Hs movements, respectively. Knight and Fuchs (2007) observed latencies of 31 ms for the Es and 60 ms for Hs when they stimulated at a frequency of 350 Hz. They also tested 200-Hz frequencies that yielded latencies of 50 ms for the Es and 74 ms for Hs. Elsley et al. (2007) reported 40 and 73 ms for the Es and the Hs, respectively. In the case of Chen's study, values of 91 ms for the Es and 179 ms for the Hs were reported in one experimental condition; in a different experimental condition he also reported 81 ms for Es and 178 ms for Hs. Here we recorded mean Es latencies of 68 ms (median = 58) for both monkeys and 79 ms (median = 70) for the Hs. Taking into account latencies of both the Es and the Hs our values are in closest agreement with the values reported by Knight and Fuchs when they used 200-Hz stimulation frequencies (in our study we used frequencies of 300 Hz).

In the study of Chen (2006), the electrical stimulations evoked small head movements in which the head movement latency lagged gaze latency by >80 ms. One possible difference between our study and that of Chen that could explain these differences is that the animals in the Chen study were trained to separately align eye and head positions. Although this approach is useful when discerning initial position dependencies it may have modified or biased the kinematics of the head movements. This possibility is prompted by studies showing that electrically evoked movements can be altered by task demands and/or cognitive variables (Fujii et al. 1995; Gold and Shadlen 2000; Tehovnik and Slocum 2000). Another possibility that could explain the differences between studies is that different animals could have different eye–head coordination strategies during natural gaze shifts and in turn this could affect the stimulation-evoked eye–head kinematics. This phenomenon has been described in human behavior; different individuals can be classified as head movers and nonhead movers when performing the same visuomotor task (Fuller 1992; Stahl 2001).

Another difference between the current study and previous studies is that varying the duration of the stimulation trains did not produce any discernable trend in increasing the Hs or Es amplitude (Supplemental Fig. S2). However, in FEF stimulation-evoked trials an increment in Es, Hs, and Eh amplitude has

been reported with longer durations of stimulation trains (Knight and Fuchs 2007). A potential reason for this discrepancy between studies is that we purposefully excluded sites that coded mainly for multistep gaze shifts; we also excluded occasional multistep gaze shifts from our analysis (see METHODS). Knight and Fuchs (2007) used the "first step" of the multiple-step gaze shifts to perform their analysis. Alternatively, initial position dependencies are also known to affect the amplitude of stimulation-evoked movements in the FEF (Knight and Fuchs 2007). Differences in initial positions between our study and previous studies could have played a role in the relation between train duration and movement amplitude.

As in previous studies we used a standard train duration of 200 ms (Knight and Fuchs 2007; Tu and Keating 2000). This was selected because it has been shown that this train duration evokes eye–head movements similar to those encountered during natural gaze shifts and reliable head movements (Knight and Fuchs 2007; Tu and Keating 2000). In this way, the evoked latencies began shortly after stimulation onset and could end before or after the end of stimulation. These raise the possibility that some of these movements, particularly those with medium or large amplitudes, could have been truncated due to cessation of stimulation (Freedman et al. 1996). However, when we controlled for different stimulation train durations (Supplemental Fig. S2), we found no trend of amplitude increments as a function of increments in train duration. These suggest that movement truncation is not substantial in our data.

Our results support the notion that there is some degree of topographical organization in the FEF. However, this organization seems rather poor when compared with other oculomotor structures like the SC (Guitton et al. 1980; Klier et al. 2001; Robinson 1972; Schiller and Koerner 1971). The general agreement is that FEF sites coding small-amplitude saccades/gaze shifts are located in posterior (caudal) areas, whereas sites coding larger amplitudes are located in anterior (rostral) areas (Bruce et al. 1985; Chen 2006; Fukushima et al. 2000; Knight and Fuchs 2007). Our results support these previous observations (see CV values for stimulation sites in Fig. 1, *A–D*), particularly in M1.

The exception to this trend was a small cluster of sites located in more posterior areas; these sites were found on the right FEF of M1. These sites coded extremely large gaze shifts (CV $>50°$, Fig. 1) where the head rotation was the main component of the gaze shifts (Fig. 3 and Supplemental Fig. S3). Although we explored the same general location in M2, we were not able to find sites coding for similar amplitudes. In the latter case, perhaps our electrode probes simply missed the location of these types of sites. Another explanation may be intraspecies differences between our monkeys; as mentioned earlier, it is known that differences exist in human head movement kinematics (Fuller 1992; Stahl 2001). It is likely that this same variability is found in other primate species as well. The intraspecies differences as an explanation of this phenomenon is further supported by the rest of our analysis that in general shows the same trend for both monkeys, but with one of the animals exhibiting a scaled (lower values) version of the values (Figs. 1, 3, and 5).

It is also possible that at our large-amplitude sites the electrode stimulated white matter fibers, yielding a motor output from other gaze-related centers. However, these options seem unlikely for two reasons: first, the mentioned sites had depths between 3.5 and 4.5 mm below the dura matter (Fig. 1). Second, we used low-threshold currents to identify the FEF, a methodology that has produced stable results in numerous studies and has become the standard means of functionally defining the FEF (Bruce et al. 1985; Chen 2006; Elsley et al. 2007; Gold and Shadlen 2000; Knight and Fuchs 2007; Schall and Hanes 1993).

Implications for 3D gaze control

A central question concerning gaze control is the degree to which the eye and head are controlled by common (Galiana and Guitton 1992; Guitton et al. 2003) or independent (Freedman 2001; Freedman and Sparks 1997; Kardamakis and Moschovakis 2009; Kardamakis et al. 2010; Phillips et al. 1995) mechanisms. Currently, most investigators favor an intermediate view in which the eye and head are guided by interacting control signals (Freedman 2001; Kardamakis and Moschovakis 2009; Kardamakis et al. 2010; Monteon et al. 2005; Tweed 1997). However, the fundamental question remains, of how a single sensory signal is elaborated to control two coordinated effectors (the eye and head) while maintaining the overall goal of fixating the target. A closely related question—examined here for the first time in the FEF— is: at what point in the brain are commands for desired 2D gaze direction elaborated into commands for 3D rotations of the eyes and head (Crawford et al. 2003)?

A number of authors have approached this question by stimulating the brain and then observing whether this produces a gaze command that is decomposed into eye and head commands according to the natural rules of eye–head coordination or independent eye and head commands that do not follow these rules (Chen 2006; Constantin et al. 2009; Freedman et al. 1996; Guillaume and Pelisson 2001; Klier et al. 2003; Knight and Fuchs 2007; Martinez-Trujillo et al. 2003b). Knight and Fuchs (2007) have applied this method to the FEF and found results generally similar to ours, but we are the first to combine this with 3D recordings of the eye and head. With the exception of Chen (2006) and one site in the FEF of the present study, the findings of these experiments and ours are generally consistent with the hypothesis that the FEF encodes 2D gaze commands that are then elaborated into complete, coordinated movements by other structures. Overall, the nature of the FEF motor commands possess all the kinematic characteristics of a naturally occurring movement. Not only on the amplitude–velocity and relative head contribution to gaze profiles, but also in the intricate 3D kinematics constrained by Donders' law, Listing's law, and its variations.

Although our results agree with previous results from the SEF (Martinez-Trujillo et al. 2003b) and superior colliculus (Klier et al. 2003), they cannot be argued away as trivial. First, microstimulation of the midbrain reticular formation produces torsional rotations that violate Donder's laws of both the eyes and head (Crawford et al. 1991; Klier et al. 2007). Second, we have recently found that stimulation of the LIP produces eye movements (including eye-in-head torsion) that are *not* accompanied by the normally coordinated pattern of head movement or return movements to Listing's plane (Constantin et al. 2009). However, since LIP is functionally upstream from FEF, SEF, and SC—all of which do produce kinematically normal

gaze shifts—this result is likely due to an *absence* of direct influence over the motor circuitry, rather than an independent oculomotor drive. Third, here we found one site in the left FEF of one monkey that produced large, consistent torsional head movements (Supplemental Fig. S6), although we could not establish whether this site was related to gaze control. It is not possible to withdraw any firm conclusions based on such an anecdotal finding, but this provides the exception that proves the rule, and an existence proof that there are cortical sites that encode 3D head movement.

Further experiments are required to determine the cortical mechanisms for movements that do not obey Donder's law (Crawford et al. 1999, 2003; Donders 1848; Glenn and Vilis 1992). For example, Donder's law of the head is modified or abandoned under different behavioral conditions (Ceylan et al. 2000). Moreover, one can freely violate Donders' law of the head at will, and even Donders' law of the eye can be voluntarily violated with training (Balliet and Nakayama 1978). Clearly, head torsion is used for some nongaze behaviors, such as gesturing and biting. These factors suggest that the high-level control mechanisms for torsion exist, perhaps parallel to the gaze control system.

Finally, there is also evidence for independent head control of the eye and head at the cortical level. Some FEF neurons have been shown to encode head movements independent of gaze shifts (Bizzi and Schiller 1970) and FEF stimulation can evoke head-only movements (Chen 2006; Elsley et al. 2007; Knight and Fuchs 2007). Moreover, when monkeys were physically constrained to make gaze shifts with larger head movements, stimulation of the SC evoked adapted eye movements, but not head movements, suggesting that a parallel cortical input is required for this behavior (Constantin et al. 2004). Several studies support the existence of independent channels from frontal cortex to the brain stem (Chen 2006; Segraves 1992; Sparks and Hartwich-Young 1989; van Opstal et al. 1991). Finally, SC neurons may also encode separate head movement signals (Walton et al. 2007), although it is not clear whether these play a causal role in gaze control (Walton et al. 2008). Our data do not contradict these results and all of these findings can be fit within the general framework of models that divide sensory signals into separate, but interacting, eye and head commands (Freedman 2001; Kardamakis and Moschovakis 2009; Kardamakis et al. 2010; Monteon et al. 2005; Tweed 1997).

In conclusion, we believe the simplest explanation for our results is that most sites in the FEF, and other similar gaze control centers, encode an undifferentiated 2D gaze signal, relayed to the 2D gaze map of the SC (Constantin et al. 2009; Klier et al. 2003; Komatsu and Suzuki 1985; Martinez-Trujillo et al. 2003b; Sommer and Wurtz 2000; van Opstal et al. 1991) and then further elaborated into 3D eye and head commands at the level of the reticular formation and cerebellum (Crawford et al. 2003; Straumann and Zee 1995). Activation of these circuits through microstimulation appears to produce a default level of eye–head coordination for the "typical" gaze shift.

GRANTS

This work was supported by the Canadian Institutes of Health Research, the Natural Sciences and Engineering Research Council of Canada, and a Consejo Nacional de Ciencia y Tecnología de México grant to J. A. Monteon. J. D. Crawford holds a Canada Research Chair.

DISCLOSURES

No conflicts of interest, financial or otherwise, are declared by the authors.

REFERENCES

Andersen RA, Asanuma C, Cowan WM. Callosal and prefrontal associational projecting cell populations in area 7A of the macaque monkey: a study using retrogradely transported fluorescent dyes. *J Comp Neurol* 232: 443–455, 1985.

Balliet R, Nakayama K. Training of voluntary torsion. *Invest Ophthalmol Vis Sci* 17: 303–314, 1978.

Bizzi E, Kalil RE, Tagliasco V. Eye–head coordination in monkeys: evidence for centrally patterned organization. *Science* 173: 452–454, 1971.

Bizzi E, Schiller PH. Single unit activity in the frontal eye fields of unanesthetized monkeys during eye and head movement. *Exp Brain Res* 10: 150–158, 1970.

Brotchie PR, Andersen RA, Snyder LH, Goodman SJ. Head position signals used by parietal neurons to encode locations of visual stimuli. *Nature* 375: 232–235, 1995.

Bruce CJ, Goldberg ME. Primate frontal eye fields. I. Single neurons discharging before saccades. *J Neurophysiol* 53: 603–635, 1985.

Bruce CJ, Goldberg ME, Bushnell MC, Stanton GB. Primate frontal eye fields. II. Physiological and anatomical correlates of electrically evoked eye movements. *J Neurophysiol* 54: 714–734, 1985.

Burke MR, Barnes GR. Brain and behavior: a task-dependent eye movement study. *Cereb Cortex* 18: 126–135, 2008.

Ceylan M, Henriques DY, Tweed DB, Crawford JD. Task-dependent constraints in motor control: pinhole goggles make the head move like an eye. *J Neurosci* 20: 2719–2730, 2000.

Chen LL. Head movements evoked by electrical stimulation in the frontal eye field of the monkey: evidence for independent eye and head control. *J Neurophysiol* 95: 3528–3542, 2006.

Chen LL, Tehovnik EJ. Cortical control of eye and head movements: integration of movements and percepts. *Eur J Neurosci* 25: 1253–1264, 2007.

Constantin AG, Wang H, Crawford JD. Role of superior colliculus in adaptive eye–head coordination during gaze shifts. *J Neurophysiol* 92: 2168–2184, 2004.

Constantin AG, Wang H, Monteon JA, Martinez-Trujillo JC, Crawford JD. Three-dimensional eye–head coordination in gaze shifts evoked during stimulation of the lateral intraparietal cortex. *Neuroscience* 164: 1284–1302, 2009.

Crawford JD, Cadera W, Vilis T. Generation of torsional and vertical eye position signals by the interstitial nucleus of Cajal. *Science* 252: 1551–1553, 1991.

Crawford JD, Ceylan MZ, Klier EM, Guitton D. Three-dimensional eye–head coordination during gaze saccades in the primate. *J Neurophysiol* 81: 1760–1782, 1999.

Crawford JD, Guitton D. Visual-motor transformations required for accurate and kinematically correct saccades. *J Neurophysiol* 78: 1447–1467, 1997.

Crawford JD, Martinez-Trujillo JC, Klier EM. Neural control of three-dimensional eye and head movements. *Curr Opin Neurobiol* 13: 655–662, 2003.

Crawford JD, Vilis T. Axes of eye rotation and Listing's law during rotations of the head. *J Neurophysiol* 65: 407–423, 1991.

Delreux V, Vanden Abeele S, Lefèvre P, Roucoux A. Eye-head co-ordination: influence of eye position on the control of head movement amplitude. In: *Brain and Space*, edited by Paillard J. Oxford, UK: Oxford Univ. Press, 1991, p. .38–48

Donders FC. Beitrag sur Lehre von den Bewegungen des menschlichen Auges. *Holland Beitr Anat Physiol Wiss* 1: 105–145, 1848.

Elsley JK, Nagy B, Cushing SL, Corneil BD. Widespread presaccadic recruitment of neck muscles by stimulation of the primate frontal eye fields. *J Neurophysiol* 98: 1333–1354, 2007.

Farshadmanesh F, Chang P, Wang H, Yan X, Corneil BD, Crawford JD. Neck muscle synergies during stimulation and inactivation of the interstitial nucleus of Cajal (INC). *J Neurophysiol* 100: 1677–1685, 2008.

Ferman L, Collewijn H, Van den Berg AV. A direct test of Listing's law—I. Human ocular torsion measured in static tertiary positions. *Vision Res* 27: 929–938, 1987a.

Ferman L, Collewijn H, Van den Berg AV. A direct test of Listing's law—II. Human ocular torsion measured under dynamic conditions. *Vision Res* 27: 939–951, 1987b.

Freedman EG. Interactions between eye and head control signals can account for movement kinematics. *Biol Cybern* 84: 453–462, 2001.

Freedman EG, Sparks DL. Eye–head coordination during head-unrestrained gaze shifts in rhesus monkeys. *J Neurophysiol* 77: 2328–2348, 1997.

Freedman EG, Stanford TR, Sparks DL. Combined eye–head gaze shifts produced by electrical stimulation of the superior colliculus in rhesus monkeys. *J Neurophysiol* 76: 927–952, 1996.

Fujii N, Mushiake H, Tamai M, Tanji J. Microstimulation of the supplementary eye field during saccade preparation. *Neuroreport* 6: 2565–2568, 1995.

Fukushima K, Sato T, Fukushima J, Shinmei Y, Kaneko CR. Activity of smooth pursuit-related neurons in the monkey periarcuate cortex during pursuit and passive whole-body rotation. *J Neurophysiol* 83: 563–587, 2000.

Fuller JH. Head movement propensity. *Exp Brain Res* 92: 152–164, 1992.

Galiana HL, Guitton D. Central organization and modeling of eye-head coordination during orienting gaze shifts. *Ann NY Acad Sci* 656: 452–471, 1992.

Glenn B, Vilis T. Violations of Listing's law after large eye and head gaze shifts. *J Neurophysiol* 68: 309–318, 1992.

Gold JI, Shadlen MN. Representation of a perceptual decision in developing oculomotor commands. *Nature* 404: 390–394, 2000.

Guillaume A, Pelisson D. Gaze shifts evoked by electrical stimulation of the superior colliculus in the head-unrestrained cat. I. Effect of the locus and of the parameters of stimulation. *Eur J Neurosci* 14: 1331–1344, 2001.

Guitton D. Control of eye-head coordination during orienting gaze shifts. *Trends Neurosci* 15: 174–179, 1992.

Guitton D, Bergeron A, Choi WY, Matsuo S. On the feedback control of orienting gaze shifts made with eye and head movements. *Prog Brain Res* 142: 55–68, 2003.

Guitton D, Crommelinck M, Roucoux A. Stimulation of the superior colliculus in the alert cat. I. Eye movements and neck EMG activity evoked when the head is restrained. *Exp Brain Res* 39: 63–73, 1980.

Guitton D, Munoz DP, Galiana HL Gaze control in the cat: studies and modeling of the coupling between orienting eye and head movements in different behavioral tasks. *J Neurophysiol* 64: 509–531, 1990.

Histed MH, Bonin V, Reid RC. Direct activation of sparse, distributed populations of cortical neurons by electrical microstimulation. *Neuron* 63: 508–522, 2009.

Huerta MF, Krubitzer LA, Kaas JH. Frontal eye field as defined by intracortical microstimulation in squirrel monkeys, owl monkeys, and macaque monkeys. II. Cortical connections. *J Comp Neurol* 265: 332–361, 1987.

Kardamakis AA, Grantyn A, Moschovakis AK. Neural network simulations of the primate oculomotor system. V. Eye-head gaze shifts. *Biol Cybern* 102: 209–225, 2010.

Kardamakis AA, Moschovakis AK. Optimal control of gaze shifts. *J Neurosci* 29: 7723–7730, 2009.

Klier EM, Crawford JD. Neural control of three-dimensional eye and head posture. *Ann NY Acad Sci* 1004: 122–131, 2003.

Klier EM, Wang H, Crawford JD. The superior colliculus encodes gaze commands in retinal coordinates. *Nat Neurosci* 4: 627–632, 2001.

Klier EM, Wang H, Crawford JD. Three-dimensional eye–head coordination is implemented downstream from the superior colliculus. *J Neurophysiol* 89: 2839–2853, 2003.

Klier EM, Wang H, Crawford JD. Interstitial nucleus of Cajal encodes three-dimensional head orientations in Fick-like coordinates. *J Neurophysiol* 97: 604–617, 2007.

Knight TA, Fuchs AF. Contribution of the frontal eye field to gaze shifts in the head-unrestrained monkey: effects of microstimulation. *J Neurophysiol* 97: 618–634, 2007.

Komatsu H, Suzuki H. Projections from the functional subdivisions of the frontal eye field to the superior colliculus in the monkey. *Brain Res* 327: 324–327, 1985.

Martinez-Trujillo JC, Klier EM, Wang H, Crawford JD. Contribution of head movement to gaze command coding in monkey frontal cortex and superior colliculus. *J Neurophysiol* 90: 2770–2776, 2003a.

Martinez-Trujillo JC, Wang H, Crawford JD. Electrical stimulation of the supplementary eye fields in the head-free macaque evokes kinematically normal gaze shifts. *J Neurophysiol* 89: 2961–2974, 2003b.

McCluskey MK, Cullen KE. Eye, head, and body coordination during large gaze shifts in rhesus monkeys: movement kinematics and the influence of posture. *J Neurophysiol* 97: 2976–2991, 2007.

Misslisch H, Tweed D, Vilis T. Neural constraints on eye motion in human eye–head saccades. *J Neurophysiol* 79: 859–869, 1998.

Monteon JA, Avillac M, Wang H, Yan X, Crawford JD. Cognitive aspects of eye-head coordination: role of frontal eye fields and superior colliculus. *Soc Neurosci Abstr* 19.9, 2007.

Monteon JA, Martinez-Trujillo JC, Wang H, Crawford JD. Cross-coupled adaptation of eye and head position commands in the primate gaze control system. *Neuroreport* 16: 1189–1192, 2005.

Moore T, Armstrong KM. Selective gating of visual signals by microstimulation of frontal cortex. *Nature* 421: 370–373, 2003.

Murphey DK, Maunsell JH. Electrical microstimulation thresholds for behavioral detection and saccades in monkey frontal eye fields. *Proc Natl Acad Sci USA* 105: 7315–7320, 2008.

Nyffeler T, Wurtz P, Luscher HR, Hess CW, Senn W, Pflugshaupt T, von Wartburg R, Luthi M, Muri RM. Repetitive TMS over the human oculomotor cortex: comparison of 1-Hz and theta burst stimulation. *Neurosci Lett* 409: 57–60, 2006.

Oommen BS, Smith RM, Stahl JS. The influence of future gaze orientation upon eye-head coupling during saccades. *Exp Brain Res* 155: 9–18, 2004.

Phillips JO, Ling L, Fuchs AF, Siebold C, Plorde JJ. Rapid horizontal gaze movement in the monkey. *J Neurophysiol* 73: 1632–1652, 1995.

Radau P, Tweed D, Vilis T. Three-dimensional eye, head, and chest orientations after large gaze shifts and the underlying neural strategies. *J Neurophysiol* 72: 2840–2852, 1994.

Ranck JB Jr. Which elements are excited in electrical stimulation of mammalian central nervous system: a review. *Brain Res* 98: 417–440, 1975.

Robinson DA. Eye movements evoked by collicular stimulation in the alert monkey. *Vision Res* 12: 1795–1808, 1972.

Robinson DA, Fuchs AF. Eye movements evoked by stimulation of frontal eye fields. *J Neurophysiol* 32: 637–648, 1969.

Russo GS, Bruce CJ. Effect of eye position within the orbit on electrically elicited saccadic eye movements: a comparison of the macaque monkeys' frontal and supplementary eye fields. *J Neurophysiol* 69: 800–818, 1993.

Schall JD. Visuomotor areas of the frontal lobe. In: *Cerebral Cortex*, edited by Rockland AP, Kaas J. New York: Plenum Press, 1997, p. 527–638.

Schall JD, Hanes DP. Neural basis of saccade target selection in frontal eye field during visual search. *Nature* 366: 467–469, 1993.

Schall JD, Hanes DP, Thompson KG, King DJ. Saccade target selection in frontal eye field of macaque. I. Visual and premovement activation. *J Neurosci* 15: 6905–6918, 1995a.

Schall JD, Morel A, King DJ, Bullier J. Topography of visual cortex connections with frontal eye field in macaque: convergence and segregation of processing streams. *J Neurosci* 15: 4464–4487, 1995b.

Schall JD, Thompson KG. Neural selection and control of visually guided eye movements. *Annu Rev Neurosci* 22: 241–259, 1999.

Schiller PH, Koerner F. Discharge characteristics of single units in superior colliculus of the alert rhesus monkey. *J Neurophysiol* 34: 920–936, 1971.

Schiller PH, Sandell JH. Interactions between visually and electrically elicited saccades before and after superior colliculus and frontal eye field ablations in the rhesus monkey. *Exp Brain Res* 49: 381–392, 1983.

Segraves MA. Activity of monkey frontal eye field neurons projecting to oculomotor regions of the pons. *J Neurophysiol* 68: 1967–1985, 1992.

Sommer MA, Wurtz RH. Composition and topographic organization of signals sent from the frontal eye field to the superior colliculus. *J Neurophysiol* 83: 1979–2001, 2000.

Sparks DL, Freedman EG, Chen LL, Gandhi NJ. Cortical and subcortical contributions to coordinated eye and head movements. *Vision Res* 41: 3295–3305, 2001.

Sparks DL, Hartwich-Young R. The neurobiology of saccadic eye movements. In: *Reviews of Oculomotor Research*, edited by Wurtz RH, Goldberg ME. New York: Elsevier Science, 1989, vol. 3, p. 213–255.

Stahl JS. Adaptive plasticity of head movement propensity. *Exp Brain Res* 139: 201–208, 2001.

Stanton GB, Bruce CJ, Goldberg ME. Topography of projections to posterior cortical areas from the macaque frontal eye fields. *J Comp Neurol* 353: 291–305, 1995.

Straumann D, Zee DS. Three-dimensional aspects of eye movements. *Curr Opin Neurol* 8: 69–71, 1995.

Tark KJ, Curtis CE. Persistent neural activity in the human frontal cortex when maintaining space that is off the map. *Nat Neurosci* 12: 1463–1468, 2009.

Tehovnik EJ, Slocum WM. Effects of training on saccadic eye movements elicited electrically from the frontal cortex of monkeys. *Brain Res* 877: 101–106, 2000.

Tehovnik EJ, Tolias AS, Sultan F, Slocum WM, Logothetis NK. Direct and indirect activation of cortical neurons by electrical microstimulation. *J Neurophysiol* 96: 512–521, 2006.

Thier P, Andersen RA. Electrical microstimulation distinguishes distinct saccade-related areas in the posterior parietal cortex. *J Neurophysiol* 80: 1713–1735, 1998.

Tomlinson RD. Combined eye–head gaze shifts in the primate. III. Contributions to the accuracy of gaze saccades. *J Neurophysiol* 64: 1873–1891, 1990.

Tomlinson RD, Bahra PS. Combined eye–head gaze shifts in the primate. I. Metrics. *J Neurophysiol* 56: 1542–1557, 1986a.

Tomlinson RD, Bahra PS. Combined eye–head gaze shifts in the primate. II. Interactions between saccades and the vestibuloocular reflex. *J Neurophysiol* 56: 1558–1570, 1986b.

Trageser JC, Monosov IE, Zhou Y, Thompson KG. A perceptual representation in the frontal eye field during covert visual search that is more reliable than the behavioral report. *Eur J Neurosci* 28: 2542–2549, 2008.

Tu TA, Keating EG. Electrical stimulation of the frontal eye field in a monkey produces combined eye and head movements. *J Neurophysiol* 84: 1103–1106, 2000.

Tweed D. Three-dimensional model of the human eye–head saccadic system. *J Neurophysiol* 77: 654–666, 1997.

Tweed D, Cadera W, Vilis T. Computing three-dimensional eye position quaternions and eye velocity from search coil signals. *Vision Res* 30: 97–110, 1990.

Tweed D, Haslwanter T, Fetter M. Optimizing gaze control in three dimensions. *Science* 281: 1363–1366, 1998.

Tweed D, Vilis T. Geometric relations of eye position and velocity vectors during saccades. *Vision Res* 30: 111–127, 1990.

van Opstal AJ, Hepp K, Hess BJ, Straumann D, Henn V. Two- rather than three-dimensional representation of saccades in monkey superior colliculus. *Science* 252: 1313–1315, 1991.

Volle M, Guitton D. Human gaze shifts in which head and eyes are not initially aligned. *Exp Brain Res* 94: 463–470, 1993.

von Helmholtz H. *Handbuch der physiologischen Optik*. Leipzig, Germany: L. Voss, 1867.

Walton MM, Bechara B, Gandhi NJ. Role of the primate superior colliculus in the control of head movements. *J Neurophysiol* 98: 2022–2037, 2007.

Walton MM, Bechara B, Gandhi NJ. Effect of reversible inactivation of superior colliculus on head movements. *J Neurophysiol* 99: 2479–2495, 2008.